



Article

Analysis of Optical and Near-Infrared Luminescence of Er³⁺ and Er³⁺/Yb³⁺ Co-Doped Heavy Metal Borate Glasses for Optical Amplifier Applications

Vinod Hegde ^{1,*}, G. Devarajulu ², A. G. Pramod ³ , Sangeeta B. Kolavekar ⁴, Dalal Abdullah Aloraini ⁵, Aljawhara H. Almuqrin ⁵, M. I. Sayyed ^{6,7} and G. Jagannath ⁸ 

¹ Department of Science and Humanities, PES University, BSK 3rd Stage, Bangalore 560085, India

² Department of Physics, Sri Venkateswara University, Tirupati 517502, India; deva777phy@gmail.com

³ Department of Physics, Bangalore University, Bengaluru 560056, India; pramod.virat09@gmail.com

⁴ Department of Physics, School of Advanced Sciences, KLE Technological University, Hubballi 580031, India; sangeeta_k@kletech.ac.in

⁵ Department of Physics, College of Science, Princess Nourah Bint Abdulrahman University, P.O. Box 84428, Riyadh 11671, Saudi Arabia; daalorainy@pnu.edu.sa (D.A.A.); ahalmoqren@pnu.edu.sa (A.H.A.)

⁶ Department of Physics, Faculty of Science, Isra University, Amman P.O. Box 33, Jordan; mohammed.alsyyed@iu.edu.jo

⁷ Department of Nuclear Medicine Research, Institute for Research and Medical Consultations (IRMC), Imam Abdulrahman bin Faisal University (IAU), P.O. Box 1982, Dammam 31441, Saudi Arabia

⁸ Department of Post—Graduate Studies and Research in Physics, National College, Jayanagar, Bangalore 560070, India; jagannathgreddy@gmail.com

* Correspondence: vinod.kodani@gmail.com



Citation: Hegde, V.; Devarajulu, G.; Pramod, A.G.; Kolavekar, S.B.; Aloraini, D.A.; Almuqrin, A.H.; Sayyed, M.I.; Jagannath, G. Analysis of Optical and Near-Infrared Luminescence of Er³⁺ and Er³⁺/Yb³⁺ Co-Doped Heavy Metal Borate Glasses for Optical Amplifier Applications. *Photonics* **2022**, *9*, 355.

<https://doi.org/10.3390/photonics9050355>

Received: 30 January 2022

Accepted: 6 May 2022

Published: 18 May 2022

Publisher's Note: MDPI stays neutral with regard to jurisdictional claims in published maps and institutional affiliations.



Copyright: © 2022 by the authors. Licensee MDPI, Basel, Switzerland. This article is an open access article distributed under the terms and conditions of the Creative Commons Attribution (CC BY) license (<https://creativecommons.org/licenses/by/4.0/>).

Abstract: For the near-infrared emission, Er³⁺ and Er³⁺/Yb³⁺ co-activated borate based glass hosts were synthesized by the method of melting and quenching. The emission intensity was maximum for 0.5 mol% Er³⁺ singly activated glass in the near-infrared (NIR) region covering the telecommunication window. The 2 mol% of Yb³⁺ co-doping enhanced the emission gain cross-section of the glass by two times contrast to 0.5 mol% Er³⁺ loaded glass. This enhancement shifted to lower spectral regions when P increased from 0 to 1. The effect of Yb³⁺ loading on the gain cross-section of the Er³⁺ co-activated glasses was analyzed using the McCumber theory. The results showed that the 0.5Er2Yb glass has a flat gain in the range of 1460–1640 nm, this suggest a lower pump threshold is enough to perform the laser functioning of a 1530 nm band and optical window of telecommunication applications.

Keywords: borate glasses; Er³⁺/Yb³⁺ co-doped; Judd-Ofelt theory; photoluminescence; energy transfer

1. Introduction

In the recent past, investigations on ionized rare earth (RE) ions incorporating glassy materials have received significant research interest, owing to their down-conversion and up-conversion (UC) features in infrared and infrared to visible spectral regions, which make them greatly utilized in optical amplifier, high-density optical storage, infrared converters, fiber optic communication and 3D display devices [1]. For decades, the preparation, characterization and property evaluation of REs, such as Nd³⁺ and Er³⁺ doped phosphate, borate and silicate glasses have been continued for optical gain medium application of solid-state and fiber near infra-red (NIR) lasers at 1064 and 1530 nm wavelengths [2]. These NIR lasers have been used as NIR light sources for medical as well as sensor equipment, such as LIDAR [3,4].

In particular, the trivalent erbium (Er³⁺) doped vitreous systems have received tremendous interest because of the photoluminescence (PL) emission at 1530 nm with the considerable emission cross-section and relatively long metastable time. Therefore, these

Er^{3+} activated glasses are found to be best suitable in wavelength division multiplexing (WDM) systems, microchip lasers, fiber amplifiers (EDFAs), lidar transmitters, eye-safe laser systems and waveguides [5]. In addition, the tri-valent erbium ions display luminescence in red, green and blue in the visible regions of the electromagnetic spectrum. The NIR emission intensity and related parameters of the luminescence transitions of Er^{3+} can be improved through the enhancement of corresponding transition probability, which is dependent on the surrounding ligand field of RE ions [6] for the effective utilization in the aforementioned applications. Further, because of the rapid growth in information technology, flexible networks are very much needed. To this end, the Er^{3+} doped glasses are of significant interest since the glasses can be molded into any flexible shape and size along with enhanced PL properties [6]. Furthermore, to be specific, the borate-based vitreous materials or glasses are important, owing to their wide range transparency, less processing temperatures, great thermal withstanding and excellent solubility of RE ions (reported up to 20 mol% of solubility in aluminoborate glasses [7]) compared to silicate and phosphate glasses [6]. Nonetheless, the NIR emission efficiency is highly impacted by the glass host, i.e., the energy of the phonons present in the glasses [5]. The addition of heavy metal oxides, such as PbO , Sb_2O_3 , Bi_2O_3 , GeO_2 , etc., resulted in the decrease of energy of the phonons of the glass network, thereby causing a reduction in the non-radiative relaxation rates, which this change leads to the NIR emission mechanism with ease [8]. In general, a high absorption cross-section of the absorption peaks leads to higher luminescence from the RE ion.

The weak absorption of Er^{3+} ions in near-infrared region hinders practical use in the large bandwidth NIR device fabrications. The tri-valent ytterbium ions (Yb^{3+}) possess strong absorption in NIR region compared to the Er^{3+} ion. Hence, it is predicted as a sensitizer that highly improves the efficiency of the down-conversion process of Er^{3+} ions by energy transfer [9]. In the open literature, there are many investigations revealing the energy transfer mechanisms of Er^{3+} co-doped Yb^{3+} diverse glasses, for example [5,6,10–12]. Precisely, therefore, there are many attempts at improving the NIR emission of around 1500 nm by co-doping with Yb^{3+} ions in different glass hosts [8,9,11,13]. In view of this, heavy metal borate glass can play a significant role due to its chemical, thermal and structural versatility [14]. These glasses can be prepared at a low melting temperature and it offers a high refractive index, which minimizes phonon energy and the dispersion of light in the NIR region and offer excellent moisture resistance [15]. However, there are very few reports available on improving the NIR emission efficiency of Er^{3+} ions by co-doping of Yb^{3+} ions in borate-based glasses, particularly heavy metal borate glasses.

2. Experimental and Characterization

The glass batches prepared by melt-quenching method for the present work are mentioned below:

Batch 1: $15\text{ZnO} - 10\text{Bi}_2\text{O}_3 - (75 - x)\text{B}_2\text{O}_3 - x\text{Er}_2\text{O}_3$ (where $x = 0.1, 0.5, 1$ and 2 mol%)

Batch 2: $15\text{ZnO} - 10\text{Bi}_2\text{O}_3 - (75 - x - y)\text{B}_2\text{O}_3 - x\text{Er}_2\text{O}_3 - y\text{Yb}_2\text{O}_3$ (where $y = 0.5, 1$, and 2 mol%).

For the preparation of Er_2O_3 (0.1, 0.5, 1 and 2 mol%) and Yb_2O_3 (0.5, 1 and 2 mol%) co-doped into 0.5 mol% Er^{3+} doped glasses, the molar percentage of the analytical grade oxides were weighed according to the glass batch formula mentioned above. Using agate mortar and pestle, samples were well-grounded for 30 min to homogenize the oxide mixture. Then, after, the glass mixture was transferred into a porcelain crucible and was placed inside the electrically heated muffle furnace. Initially, the furnace was set to 400°C and then slowly raised to 1000°C . For 1 h, the glass batch was heat soaked at 1000°C inside the furnace to obtain bubble-free molten liquid. Then, after 2 h of melting, the liquid glass batch was quenched on pre-annealed brass mold to obtain bulk glass pieces. These glasses were then heat treated at 273°C for 3 h and slowly cooled to standard temperature. Later, these bulk glasses were polished to get 2 mm thicknesses and were labeled as 0.1Er, 0.5Er, 1.0Er, and

2.0Er for 0.1, 0.5, 1 and 2 mol% Er_2O_3 singly loaded glasses, and co-activated glasses were labeled as 0.5Er0.5Yb, 0.5Er1.0Yb, 0.5Er2.0Yb for Er^{3+} : 0.5 mol % and Yb^{3+} : 0, 0.5, 1.0, and 2.0 mol% loaded in borate based glasses, respectively. The well-polished glasses were used for optical measurements, such as absorption, photoluminescence and decay curves. All physical parameters, are presented in Table 1. The powder form of the same glasses was used for structural characterization, such as XRD and FT-IR using an X-ray diffractometer with a 2θ range 5° to 80° and FT-IR spectra were measured from 4000 to 400 cm^{-1} . The absorption, photoluminescence and decay curves were collected utilizing a Perkin Elmer make Lambda-750 S spectrophotometer.

Table 1. The physical parameters of Er^{3+} singly loaded studied glasses.

Physical Parameters	0.1Er	0.5Er	1.0Er	2.0Er
Density (g/cm^3)	3.31	3.45	3.59	3.70
Thickness (cm)	0.152	0.154	0.153	0.151
Refractive index (n)	1.621	1.625	1.628	1.632
Concentration N (Ions/ $\text{c.c} \times 10^{20}$)	0.156	0.903	1.963	3.938

3. Results and Discussion

The XRD profiles of Er^{3+} singly loaded glasses are shown in Figure 1. The XRD profiles of the glasses showed broad humps without any sharp crystallographic peaks. The absence of such crystallographic peaks insisted that the prepared glass samples possess an amorphous network in them [16].

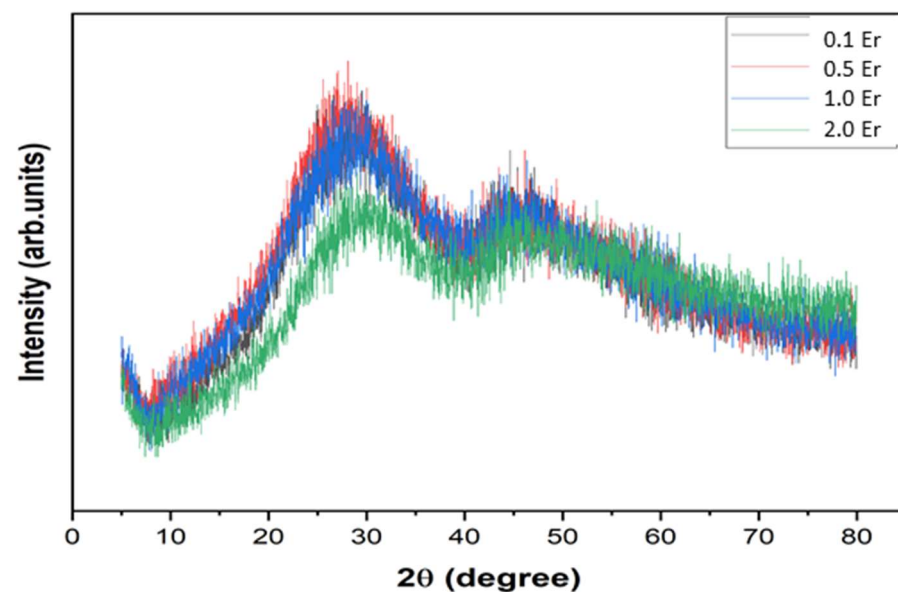


Figure 1. XRD of Er_2O_3 doped ZBB glasses.

The features of the FT-IR absorption spectra of the Er_2O_3 doped 15ZnO , $10\text{Bi}_2\text{O}_3$, $(75 - x)\text{B}_2\text{O}_3$, and $x\text{Er}_2\text{O}_3$ were recorded with the resolution of 4 cm^{-1} . The powdered form of the samples was palletized using KBr as a binder and, then, it was used to measure the absorption mode of the FT-IR spectra in the infrared region, from 400 to 4000 cm^{-1} . Figure 2 consists of absorption broad bands of the vitreous network of Er^{3+} doped glasses. The demonstrated band in the spectra, around 441 to 579 cm^{-1} , was attributable to the formation of the octahedral BiO_6 group in the vitreous network [17,18]. Additionally, the formation of the BO_3 groups in the borate structure absorbed the energy for its in-plane bending vibrations at the same wavenumber, 441 to 579 cm^{-1} [19]. The broad FT-IR band ranging from 638 to 746 cm^{-1} is manifested to bending motion of B–O bonds exist in the BO_3 units [19]. The FT-IR signature between 787 – 1046 cm^{-1} , is caused because of the

motion of B–O bonds' in the BO_4 motifs [20]. The partial portion of the fourth FT-IR band, from 1144 to 1286 cm^{-1} , has owed to the B–O bond's stretch in the $(\text{BO}_3)^{3-}$ functional groups [20]. The other half of the band is in the range of 1301 to 1478 cm^{-1} because of the stretch of B–O bonds of $(\text{BO}_3)^{3-}$ groups, which are an integral part of the synthesized vitreous glass network [20]. The structure of bismuth zinc borate glasses has not been modified due to the addition of Er^{3+} concentration.

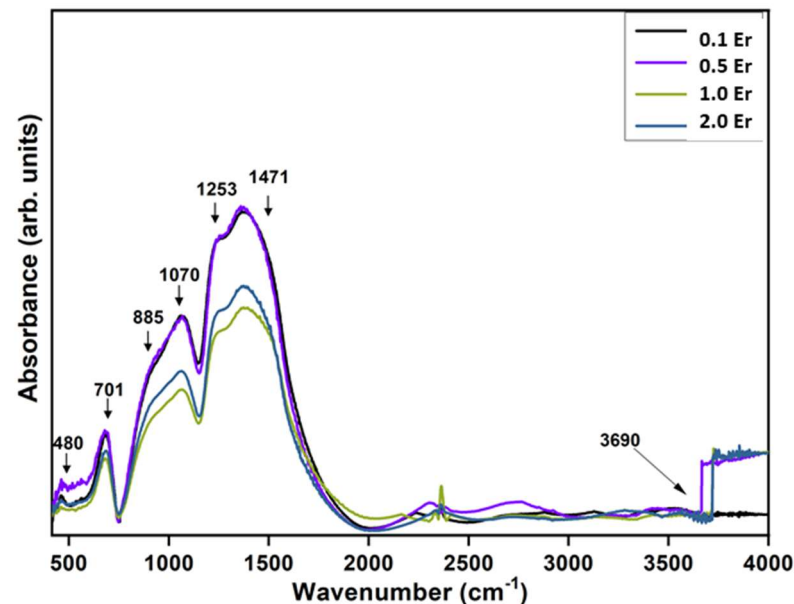


Figure 2. FT-IR spectral results of studied Er_2O_3 doped ZBB glasses.

Linear absorption spectral results of Er^{3+} singly activated glasses depicted in Figure 3 for UV-visible region (upper figure) and NIR region (below figure). The Er^{3+} ions showed their electronic transitions from their lower energy level ($^4\text{I}_{15/2}$) to the different higher energy levels. All the peaks observed for the singly Er^{3+} doped glass samples used in the current study are assigned by referring to the reference [21]. From the spectra, it can be seen that, the intensity of the bands is enhanced monotonously with respect to Er^{3+} content in the composition. Among all transitions, the $^4\text{I}_{15/2} \rightarrow ^2\text{H}_{11/2}$ possess highest intensity and is hypersensitive transition [HST], whose intensity sensitive to the surrounding structure [22]. Figure 4 displays the optical absorption spectra of 0.5Er (single) and co-doped (Er/Yb) in UV-vis–NIR (350–1700 nm) regions. Figure 4 shows the additional intense absorption band at 977 nm and it was ascribed to the $\text{Yb}^{3+}: ^2\text{F}_{7/2} \rightarrow ^2\text{F}_{5/2}$ transition in all co-doped glasses [23–25]. Absorption at 977 nm ($^2\text{F}_{7/2} \rightarrow ^2\text{F}_{5/2}$) significantly increased with the increment of Yb^{3+} ions from 0.5 to 2.0 mol% in the Er/Yb multiple RE ions doped glasses. Interestingly, the spectra revealed the broader absorption band around 880 to 1070 nm due to the overlap in the Yb^{3+} ions $^2\text{F}_{7/2} \rightarrow ^2\text{F}_{5/2}$ transition with the Er^{3+} ions $^4\text{I}_{15/2} \rightarrow ^4\text{I}_{11/2}$ transition. This specifies the potential of absorption efficiencies in the NIR region than the singly Er^{3+} doped glass under NIR excitation ($\lambda_{\text{exc}} = 980\text{ nm}$). The presence of co-dopant Yb^{3+} in the glass network increased the NIR, and the demonstrated broad bands are due to light absorption glass around 980 nm.

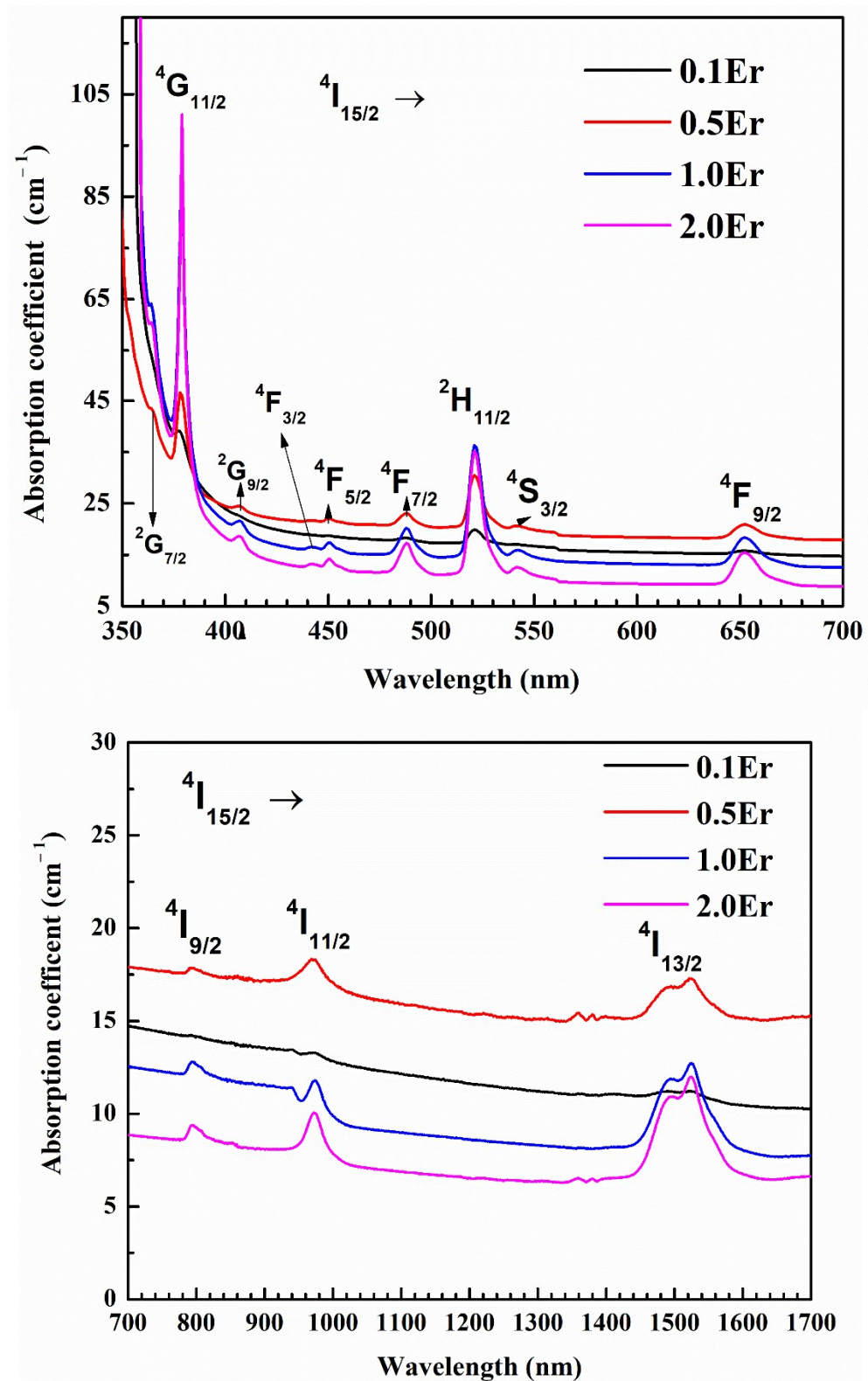


Figure 3. Optical absorption spectra of UV-vis (350–700 nm) (upper) and NIR (700–1700 nm) (lower) of Er³⁺ singly activated ZBB glasses.

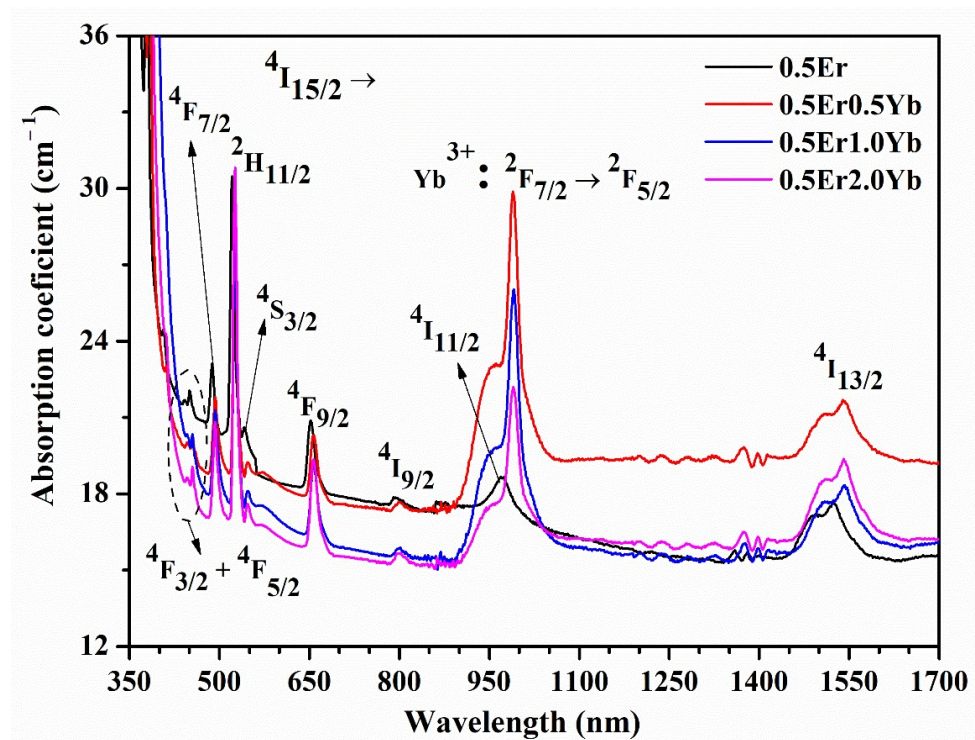


Figure 4. Linear absorption spectral outcomes of Er³⁺/Yb³⁺ ions co-doped ZBB glasses from UV-vis to NIR (350–1700 nm) region.

Further, oscillator strengths, both f_{exp} and f_{ms} of the Er³⁺ doped glasses were computed using the relations mentioned in the references [23–25] and are tabulated in Table 2. The Judd-Ofelt (JO) factors viz. Ω_2 , Ω_4 and Ω_6 were evaluated by referring to the procedure explained in references [26,27]. Both f_{exp} and f_{cal} , along with their root mean square deviations (σ_{rms}) are furnished in Table 2. It is already proved that the JO factors describe local ligand environments around the dopants (Er³⁺ ions), and the strength of covalency between the ligand bonds. Thus, information about the site symmetry of Er³⁺ ions can be determined from Ω_2 and it is sensitive to HST, while Ω_4 and Ω_6 depend on the bulk property and viscosity of a host glass. The JO factors of singly Er-doped borate glasses are calculated and tabulated in Table 3. Among all, 0.5Er glass attain the higher values which suggest the strong covalency nature between Er-O. Further, an increase in doping of Er³⁺ into host glass reduced the strength of Ω_2 . This paramount shift is attributed to the decrease in order of symmetry around the Er³⁺ ions in in the studied glasses [22–24]. The JO parameters of the present borate glasses are comparable with SANSCer10 [5], PKSAer10 [22], fluorotellurite [23], ELB [24], TBA1 [25], TZN [28], BLK1.0Er [29], CaBaPEr20 [30], TBL [31] and lead phosphate [32] of Er³⁺ doped different glass materials.

Table 2. Experimental (f_{exp}) and calculated (f_{cal}) oscillator strengths (10^{-6}) of Er³⁺ loaded in ZBB glasses.

Transition	Energy (cm ⁻¹)	0.1Er		0.5Er		1Er		2Er	
		f_{exp}	f_{cal}	f_{exp}	f_{cal}	f_{exp}	f_{cal}	f_{exp}	f_{cal}
⁴ I _{13/2}	6527	5.41	4.67	2.33	2.67	3.22	3.52	2.93	1.05
⁴ I _{11/2}	10,256	2.46	2.72	1.56	1.23	1.17	1.61	1.33	7.17
⁴ I _{9/2}	12,516	-	-	2.66	2.70	1.07	0.92	1.30	1.72
⁴ F _{9/2}	15,361	5.65	5.89	2.91	1.11	5.39	5.71	3.53	0.84
⁴ S _{3/2}	18,416	2.25	3.67	-	-	2.65	1.35	1.83	1.45
² H _{11/2}	19,231	13.47	14.20	8.33	7.36	16.67	16.37	4.47	4.37

Table 2. Cont.

Transition	Energy (cm ⁻¹)	0.1Er		0.5Er		1Er		2Er	
		f _{exp}	f _{cal}	f _{exp}	f _{cal}	f _{exp}	f _{cal}	f _{exp}	f _{cal}
⁴ F _{7/2}	20,492	7.72	8.13	4.74	3.78	7.03	5.49	3.45	4.06
⁴ F _{5/2}	22,173	2.73	4.04	1.86	1.35	2.05	1.64	1.36	1.19
⁴ F _{3/2}	22,573	-	-	1.28	0.78	2.11	0.95	1.13	3.73
² G _{9/2}	24,631	1.58	2.49	2.15	1.56	3.08	2.03	2.97	0.47
⁴ G _{11/2}	26,525	3.16	2.85	12.02	13.05	28.77	29.02	6.73	1.23
² G _{7/2}	28,090	-	-	-	-	3.34	1.28	2.08	2.90
σ(N) ^a		±0.26 × 10 ⁻⁶		±0.85 × 10 ⁻⁶		±0.45 × 10 ⁻⁶		±0.69 × 10 ⁻⁶	

σ(N)^a shows r.m.s deviation among the f_{exp} to f_{cal} values and ‘N’ tells the number of transitions used in the fitting procedure.

Table 3. The comparison of Judd-Ofelt parameters Ω_λ (λ = 2, 4 and 6 × 10⁻²⁰ cm²) of Er³⁺ ions in different glass networks.

Glass Composition	Ω ₂	Ω ₄	Ω ₆
0.1Er (Present work)	7.28	2.76	5.09
0.5Er (Present work)	9.15	4.07	3.31
1.0Er (Present work)	4.49	2.94	2.73
2.0Er (Present work)	1.42	1.99	2.91
SANSCEr10 [5]	7.04	1.71	1.39
PKSAEr10 [22]	6.14	0.61	1.40
Florotellurite [23]	3.60	1.26	0.77
Sodium-boro-Lanthanate (ELB-1) [24]	5.96	1.96	2.04
TBA1 [25]	5.99	2.69	1.05
TZN [28]	5.96	2.42	0.53
BLK1.0Er [29]	3.19	1.38	2.16
CaBaPEr20 [30]	7.44	2.52	4.34
TBL [31]	6.17	1.50	1.10
Lead-Phosphate [32]	4.79	0.79	1.22

The NIR luminescence spectra of (0.1Er–2.0Er) doped zinc borate glasses are depicted in Figure 5. All samples emitted the broad NIR emission (1440–1680 nm) and a peak at 1529 nm (1529 nm due to electronic motion from ⁴I_{13/2} level to ⁴I_{15/2} level of Er³⁺). Thus, the NIR emission covering C and L bands of the telecommunication window thereby it can be utilized for optical amplifier applications.. Interestingly, the intensity of NIR emission enhanced with Er³⁺ doping into the glass, from 0.1 to 0.5 mol%, and beyond that intensity of the same band, was decreased. This type of decrement is caused because of agglomeration of Er³⁺ ions in the examined glass. Hence, Er³⁺ ion concentrations increase, resulting in the reduction of distance among the Er³⁺ ions and it causing the quenching process.

Further, using the JO factors, the lasing potentials, such as emission maxima (λ_p), effective line width (Δλ_{eff}), stimulated emission cross-section (σ_{emi}), branching ratio (β_R) and quantum efficiency (η) have been computed for the studied glasses by referring the procedure provided in the reference [23,24]. The resulted calculation shows values for σ_{emi} and A_T of 0.5Er glass as superior among the 0.1 to 1Er glasses. Their values are 1.52, 1.14, 0.82, 0.80 (×10⁻²¹ cm²) and 281.1, 488.14, 357.76, 304.43 (s⁻¹), respectively, corresponding to the 0.1Er, 0.5Er, 1.0Er, and 2.0Er glasses. The gain bandwidth (σ_{emi} × Δλ_{eff}) and optical gain for examined glasses are also evaluated and found to be decreased as the Er³⁺ concentration elevated to higher levels. Table 4 displays the radiative parameters of prepared glasses with other reported glasses [5,22,30–32]. The 0.5Er glasses σ_{emi} value is higher than that of reported different glass materials. Interestingly, the resulting other radiative parameters that use the emission spectra and JO parameters revealed that, the current glasses have substantial for 1530 nm broadband amplifiers and eye-safe efficient NIR lasers.

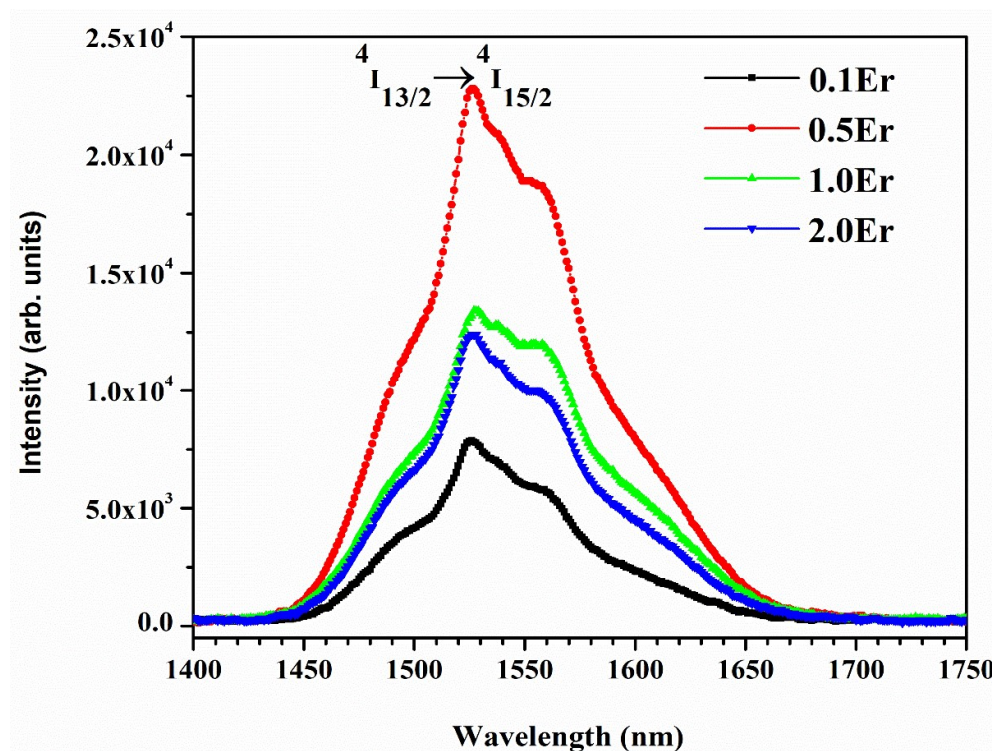


Figure 5. Near-infrared emission spectra of Er³⁺ doped ZBB glasses.

Table 4. Radiative properties for ⁴I_{13/2} → ⁴I_{15/2} of Er³⁺ ions doped ZBB glasses along with other reported glasses.

Glass Sample	A _R (s ⁻¹)	Δλ _{eff} (nm)	(β _R)	σ _{emi} (×10 ⁻²¹ cm ²)	τ _{Rad} (ms)	(σ _{emi} × Δλ _{eff}) (×10 ⁻²⁸ cm ³)	(σ _{emi} × τ _{Rad}) (×10 ⁻²⁴ cm ² s)
0.1Er (Present work)	281.1	88.98	1	15.200	3.557	1352.50	54.07
0.5Er (Present work)	488.14	86.30	1	11.412	3.284	984.86	37.48
1.0Er (Present work)	357.76	101.28	1	8.246	2.795	835.15	23.05
2.0Er (Present work)	304.43	95.75	1	8.016	2.058	767.53	16.50
SANSCEr10 [5]	193	53	1	9.8	5.18	519.4	50.76
PKSAEr10 [22]	134	34	1	6.03	7.430	204	44.02
BLK1.0Er [30]	141.89	81.21	1	8.215	7.047	667.14	57.89
CaBaPEr20 [31]	183.23	64	1	7.99	2.728	511	21.80
PKAPbNEr10 [32]	144	46	1	6.73	6.910	310	13.86

PL spectra for single (0.5Er) and co-doped samples presented in Figure 6 for an excitation of 980 nm. The spectra consist of the representative band at 1550 nm due to electronic motion from ⁴I_{13/2} to ⁴I_{15/2} levels of Er³⁺. The amplitude of this peak improved with elevation of Yb³⁺ content in the composition. Interestingly, in the co-doped glasses, Er³⁺ ions emission intensity was enhanced with the effect of Yb³⁺ ions sensitization. This enhancement is due to the strong absorption cross-section of Yb³⁺ contrast to Er³⁺ at the pumped spectral region. The pumping wavelength, energy levels and transitions profile are displayed in the energy level diagram (Figure 7).

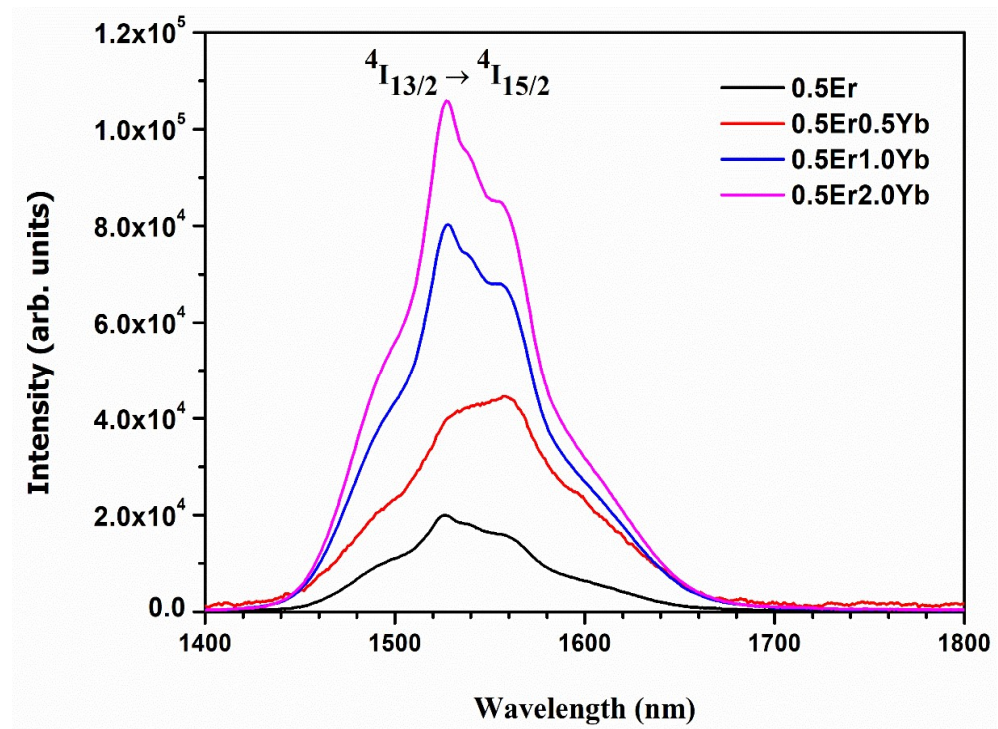


Figure 6. Near-infrared emission 0.5 mol% Er³⁺ ions and Yb³⁺ ions co-doped ZBB glasses.

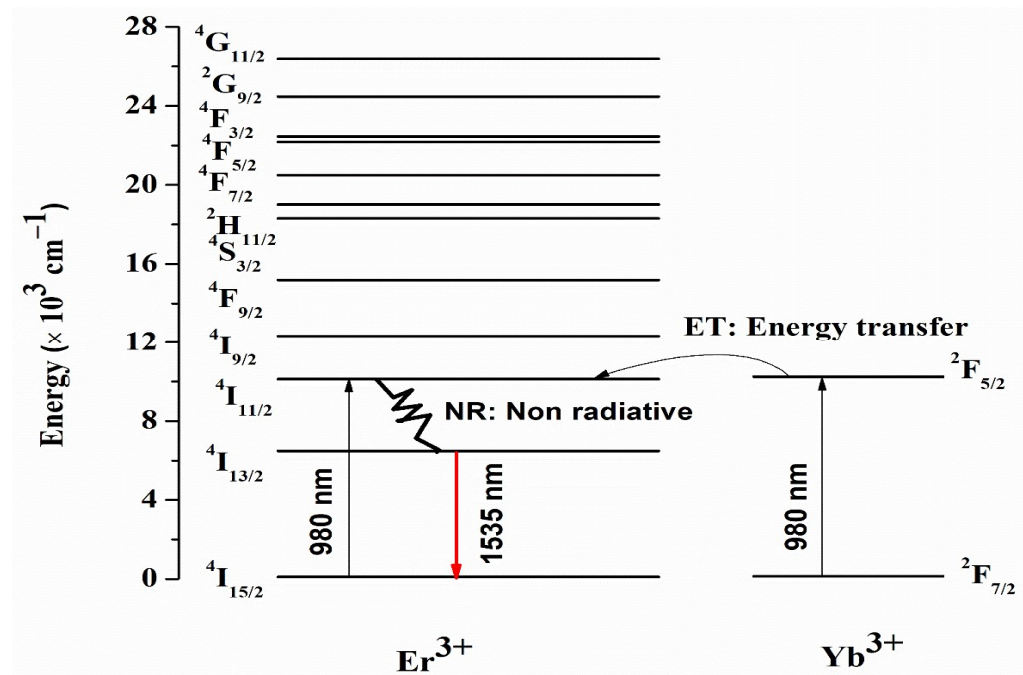


Figure 7. Energy level scheme of Er³⁺ and Yb³⁺ ions in ZBB glasses.

Further, the absorption spectrum of 0.5Er glass was utilized to compute the absorption cross-section (σ_{abs}), whilst the stimulated emission cross-section ($^M\sigma_{emi}$) was computed by following the McCumber theory (MC). The McCumber hypothesis is always referred to for explaining the overlap between the σ_{abs} and $^M\sigma_{emi}$ cross-sections. The factor of $^M\sigma_{emi}$ influences the operation of a laser and all sets of these properties were realized with the assistance of the equations provided in the references [5,29].

From McCumber’s theory, the σ_{abs} and σ_{abs} profiles of 0.5Er and 0.5Er2.0Yb co-doped glasses are shown in Figure 8a,b, respectively.

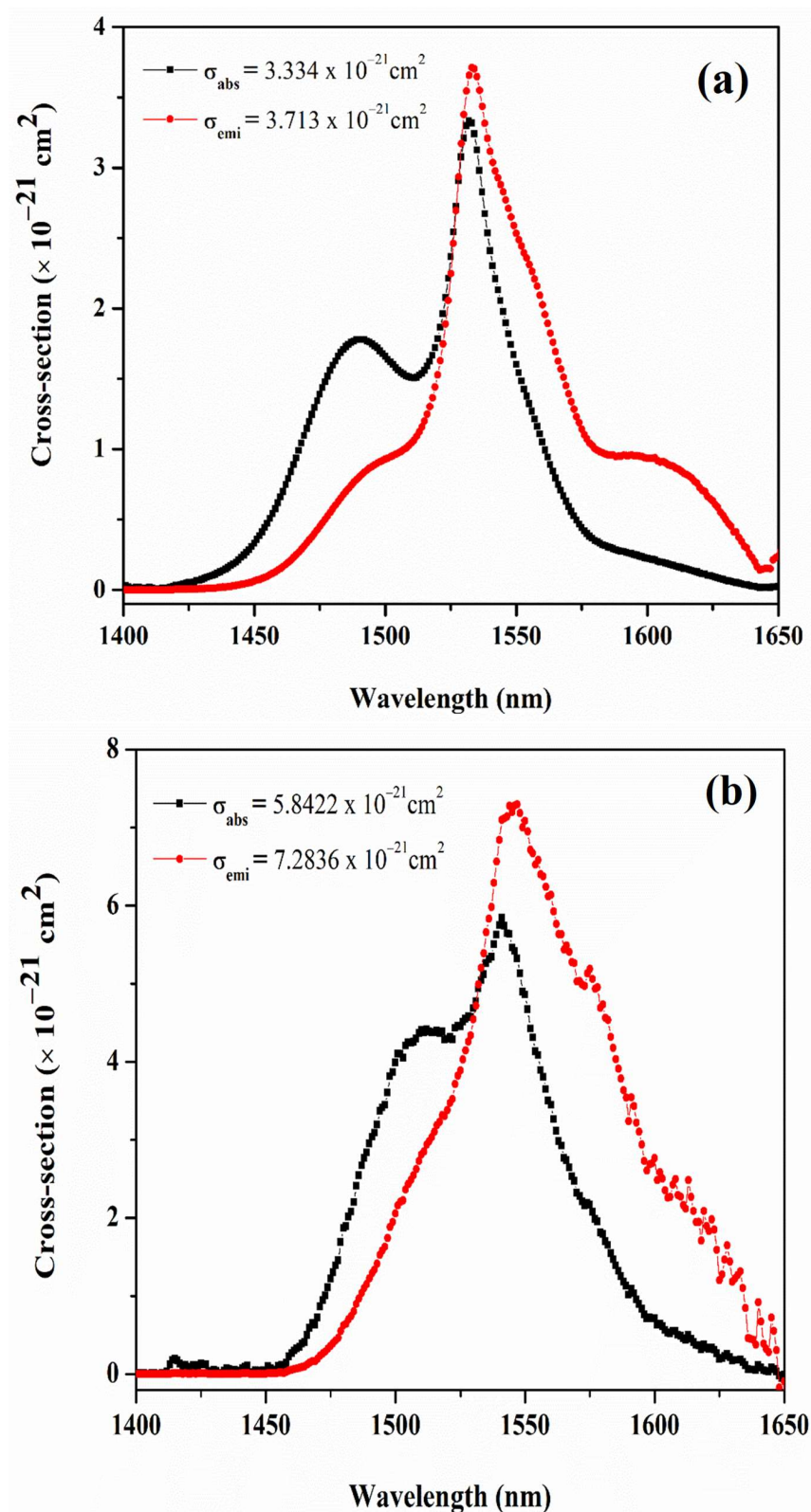


Figure 8. Absorption and emission cross-section of 0.5Er doped (a) and 0.5Er2.0Yb co-doped (b) ZBB glasses.

From Figure 8, σ_{abs} and σ_{emi} magnitudes found to be $3.334 \times 10^{-21} \text{ cm}^2$ and $3.713 \times 10^{-21} \text{ cm}^2$ respectively at $\sim 1530 \text{ nm}$ whereas which for 0.5Er2.0Yb glass the magnitudes respectively found to be $5.842 \times 10^{-21} \text{ cm}^2$ and $7.283 \times 10^{-21} \text{ cm}^2$. The σ_{emi} value is found to be the maximum ($7.283 \times 10^{-21} \text{ cm}^2$) for 0.5Er2.0Yb co-doped glasses and

was enhanced ~2 times compared that of 0.5Er glass which is attributed to the resonant transfer of energy from Yb³⁺ to Er³⁺ ions.. These values are comparable with the other reported phosphate (0.5Er/12Yb: $\sigma_{abs} = 6.15 \times 10^{-21} \text{ cm}^2$, $\sigma_{emi} = 7.11 \times 10^{-21} \text{ cm}^2$) [33], and fluorophosphate glasses (3Er4Yb: $\sigma_{abs} = 9.53 \times 10^{-21} \text{ cm}^2$, $\sigma_{emi} = 9.86 \times 10^{-21} \text{ cm}^2$) [34].

Optical gain cross-section ($G(\lambda)$) has been used to ascertain the laser media performance. The $G(\lambda)$ for ~1530 nm emission transition of 0.5Er glasses was determined by following equation [29]:

$$G(\lambda, N) = P \sigma_{emi}(\lambda) - (1 - P)\sigma_{abs}(\lambda) \tag{1}$$

where factor P is the population rate. Figure 9 exhibits the spectra of the gain cross-section $G(\lambda)$ of the 0.5Er and 0.5Er2.0Yb glasses. From the spectra, as the values of $G(\lambda)$ increase, the gain band shifts toward the short wavelength side when N increases from 0 to 1. For ~1530 nm emission transition of Er^{3+:}4I_{13/2}-⁴I_{15/2}, when N reaches 0.4, the $G(\lambda)$ achieves a magnitude of 10^{-21} cm^2 . The maximum $G(\lambda)$ is found to be $3.713 \times 10^{-21} \text{ cm}^2$ for 0.5Er and $7.2836 \times 10^{-21} \text{ cm}^2$ for 0.5Er2.0Yb glasses. $G(\lambda)$ values of 0.5Er2.0Yb glasses increased 2 times compared to 0.5Er glasses and were also related to the phosphate glasses in the range of $7.11 \times 10^{-21} \text{ cm}^2$ [33], and are less than fluorophosphate glass ($9.86 \times 10^{-21} \text{ cm}^2$) [34]. Hence, according to Figure 9, the synthesized co-doped glasses' flat gain is in the range of 1460–1640 nm. This optimum performance describes the laser operation of the 1530 nm band at a lesser pump threshold, which is a prerequisite for laser operation [29]. Hence, the obtained result infers that Er³⁺ with Yb³⁺ co-doped bismuth zinc borate glasses are competing hosts as an optical medium for laser operation at 1530 nm [31].

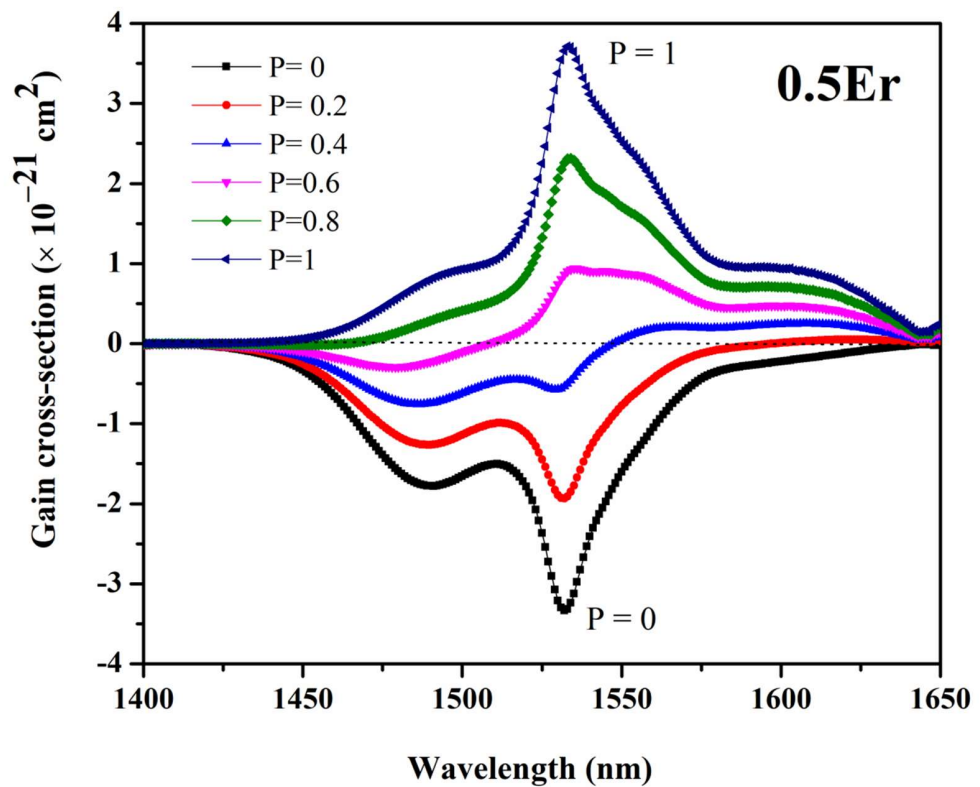


Figure 9. Cont.

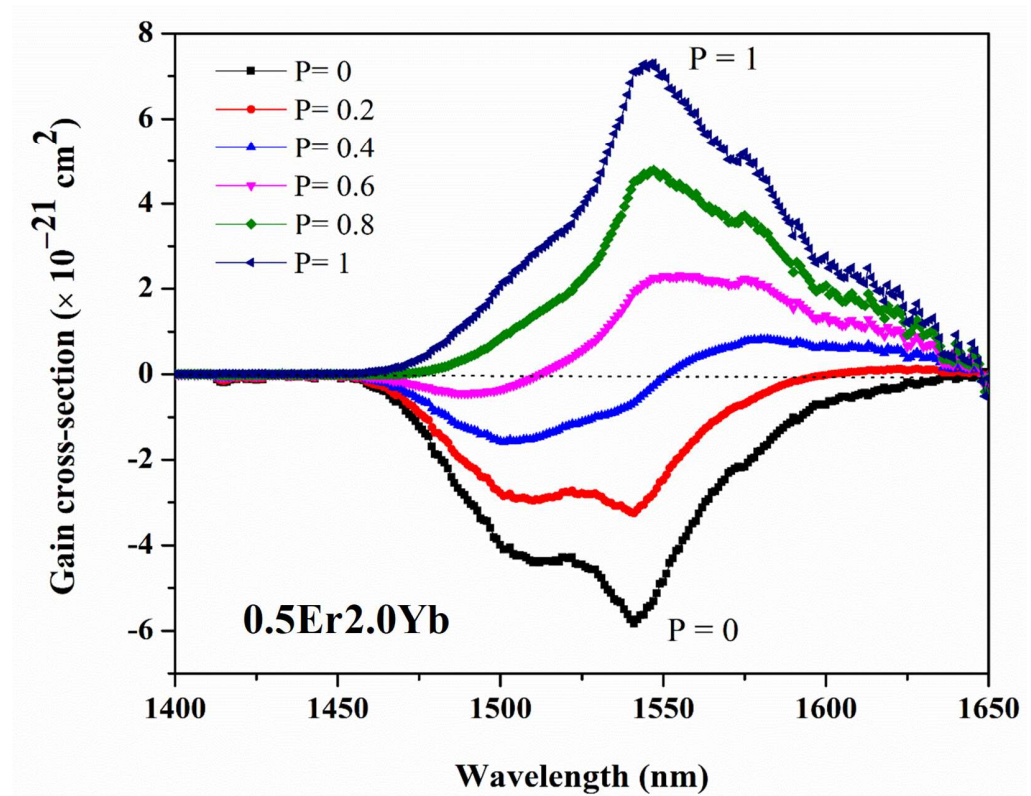


Figure 9. Gain cross-section profile of ${}^4I_{13/2} \rightarrow {}^4I_{15/2}$ transition in the range of 1400–1650 nm of 0.5Er (upper) and 0.5Er2.0Yb (lower) glasses used in the current study.

The metastable lifetime of the Er^{3+} ions plays a significant role in the EDFA and solid-state laser gain medium applications. A higher metastable lifetime eases the population inversion condition of the doped glasses. However, the lifetime of the Er^{3+} can be decreased or increased with the change in the composition of glass, doping concentration of Er^{3+} and the transfer of resonant energy from trivalent ytterbium to trivalent erbium ions [35]. Thus, the decay profiles for 0.5Er and 0.5Er/(0.5, 1.0, and 2.0)Yb co-doped ZBB glasses for ${}^4I_{13/2} \rightarrow {}^4I_{15/2}$ transition under the excitation at 976 nm provided in Figure 10. The profiles of PL decay were well fitted to single-exponential, and the obtained lifetime values are 3.56 ms, 3.60 ms, 3.99 ms, and 4.03 ms for 0.5Er, 0.5Er0.5Yb, 0.5Er1.0Yb, and 0.5Er/2.0Yb glasses, respectively. The observed behavior analogous to other $\text{Er}^{3+}/\text{Yb}^{3+}$ glass matrices were as such: $65\text{P}_2\text{O}_5\text{-}13\text{K}_2\text{CO}_3\text{-}13\text{BaCO}_3\text{-}8\text{Al}_2\text{O}_3\text{-}2\text{ZnO}$ [33]; $75\text{NaH}_2\text{PO}_4\text{-}20\text{ZnO}\text{-}5\text{Li}_2\text{CO}_3\text{-}2\text{Er}_2\text{O}_3$ [36]; $44\text{P}_2\text{O}_5\text{-}23\text{PbO}\text{-}17\text{K}_2\text{O}\text{-}9\text{Al}_2\text{O}_3\text{-}6\text{Na}_2\text{O}$ [37]. The closeness between the energy levels of ${}^4F_{5/2}$ (Yb^{3+}) to ${}^5I_{11/2}$ (Er^{3+}) ions [36] led to a high population inversion at the ${}^5I_{11/2}$ level due to transfer of resonant energy from the Yb^{3+} to Er^{3+} ions when excited at 980 nm.

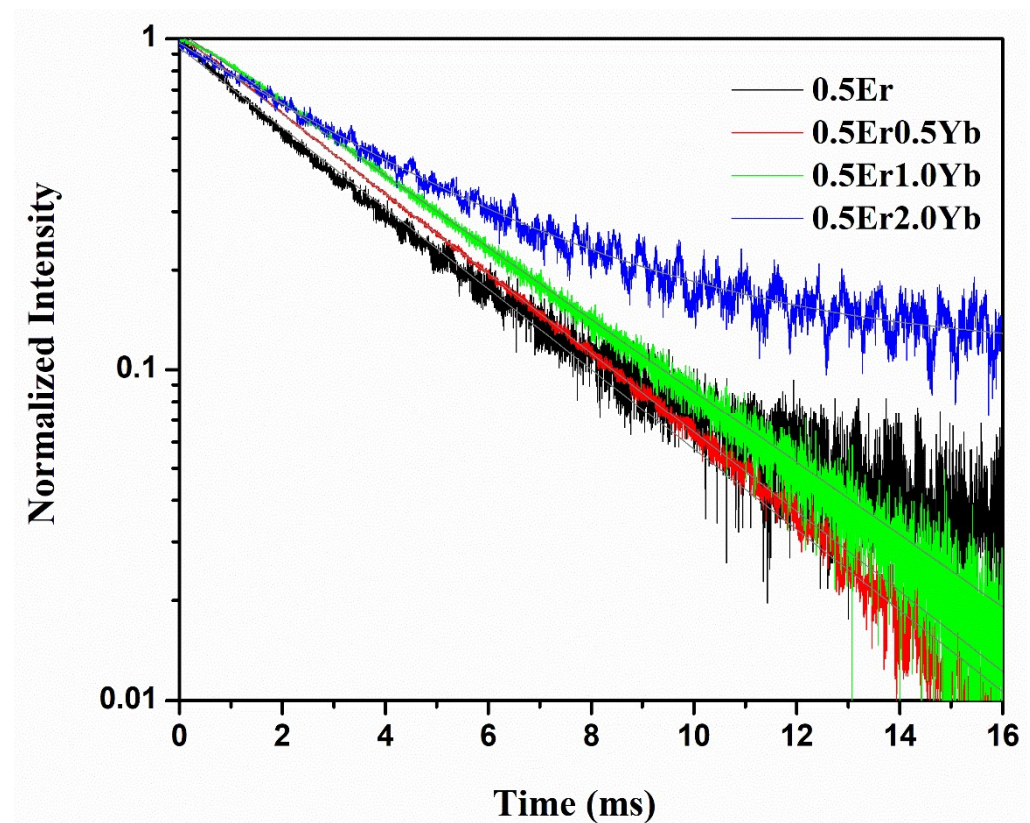


Figure 10. Decay profiles of ${}^4I_{13/2} \rightarrow {}^4I_{15/2}$ transition of 0.5Er and $\text{Er}^{3+}/\text{Yb}^{3+}$ -co-doped ZBB glasses.

4. Conclusions

In this study, the absorption spectra of the glass were observed with 12 absorption lines, with an increase of intensity with respect to Er^{3+} doping from 0.1 to 2 mol%. The addition of Yb^{3+} ion into the glass network added an extra absorption transition at 980 nm was observed. The JO factors $\Omega_2 = 9.15 \times 10^{-20}$, $\Omega_4 = 4.07 \times 10^{-20}$, and $\Omega_6 = 3.31 \times 10^{-20} \text{ cm}^2$, were the highest for 0.5 mol% Er^{3+} loaded glass; which infers the bond between Er^{3+} to O^{2-} was covalent. The NIR emission of the telecommunication window was highest in 0.5 mol% of Er^{3+} doped zinc bismuth borate glass. The obtained radiative transition probability (488.14 s^{-1}), branching ratio (1) stimulated emission cross-section ($11.41 \times 10^{-21} \text{ cm}^2$), radiative lifetime (3.2 ms), gain bandwidth ($984.86 \times 10^{-28} \text{ cm}^3$) and an optical gain ($39.48 \times 10^{-25} \text{ cm}^2\text{-s}$) of 0.5 mol% Er^{3+} loaded in borate glass suggest potential use for the construction of 1.53 μm optical amplifiers and efficient NIR lasers. Along with emission intensity, 2 mol% of Yb^{3+} co-doping enhanced the emission gain cross-section ($7.283 \times 10^{-21} \text{ cm}^2$) of the glass by two times when compared to the 0.5 mol% Er^{3+} singly doped glass network. This increase in gain cross-section shifted the gain band for lower spectral side when P increased from 0 to 1 and for the Er^{3+} : ${}^4I_{13/2} \rightarrow {}^4I_{15/2}$ emission, and when P reached 0.4, the gain cross-section achieved a magnitude of $7.283 \times 10^{-21} \text{ cm}^2$ in the 2 mol% of Yb^{3+} co-activated glass. The 0.5Er2Yb glass has a flat gain in the range of 1460–1640 nm and its behavior proved that the lower pump threshold is sufficient for laser operation within the 1530 nm band and optical window of telecommunication.

Author Contributions: V.H.: Conceptualization, Methodology, Data curation, Investigation, Writing—original draft; G.D.: Data curation, Writing—original draft; A.G.P.: Data curation, Formal analysis; S.B.K.: Data curation, Formal analysis; D.A.A.: Data curation, Writing—review & editing; A.H.A.: Data curation, Writing—review & editing; M.I.S.: Writing—review & editing; G.J.: Conceptualization, Methodology, Data curation, Writing—review & editing. All authors have read and agreed to the published version of the manuscript.

Funding: This research was funded by Princess Nourah bint Abdulrahman University Researchers Supporting Project (PNURSP2022R57), Princess Nourah bint Abdulrahman University, Riyadh, Saudi Arabia.

Institutional Review Board Statement: Not applicable.

Informed Consent Statement: Not applicable.

Data Availability Statement: All the data have been reported in the manuscript.

Acknowledgments: The authors express their gratitude to Princess Nourah bint Abdulrahman University Researchers Supporting Project (PNURSP2022R57), Princess Nourah bint Abdulrahman University, Riyadh, Saudi Arabia.

Conflicts of Interest: The authors declare no conflict of interest.

References

1. Liu, X.; Zhang, M.; Guo, R.; Liu, X.; Pan, X.; Chen, K. Deng, W. Optical properties and luminescence of Er³⁺/Yb³⁺ co-doped La₂O₃-Nb₂O₅-Ga₂O₃ glasses prepared by aerodynamic levitation method. *Opt. Mater.* **2020**, *109*, 110288. [[CrossRef](#)]
2. Chen, Y.; Huang, Y.; Huang, M.; Chen, R.; Luo, Z. Spectroscopic properties of Er³⁺ ions in bismuth borate glasses. *Opt. Mater.* **2004**, *25*, 271–278. [[CrossRef](#)]
3. Pal, I.; Sanghi, S.; Agarwal, A.; Aggarwal, M.P. Spectroscopic and structural investigations of Er³⁺ doped zinc bismuth borate glasses. *Mater. Chem. Phys.* **2012**, *133*, 151–158. [[CrossRef](#)]
4. Jose, A.; Gopi, S.; Krishnapriya, T.; Jose, T.A.; Joseph, C.; Unnikrishnan, N.V.; Biju, P.R. Spectroscopic investigations on 1.53 μm NIR emission of Er³⁺ doped multicomponent borosilicate glasses for telecommunication and lasing applications. *Mater. Chem. Phys.* **2021**, *261*, 124223. [[CrossRef](#)]
5. Devarajulu, G.; Ravi, O.; Reddy, C.M.; Ahamed, S.Z.A.; Raju, B.D.P. Spectroscopic properties and upconversion studies of Er³⁺-doped SiO₂-Al₂O₃-Na₂CO₃-SrF₂-CaF₂ oxyfluoride glasses for optical amplifier applications. *J. Lumin.* **2018**, *194*, 499–506. [[CrossRef](#)]
6. Ravi, O.; Dhoble, S.J.; Ramesh, B.; Devarajulu, G.; Reddy, C.M.; Linganna, K.; Reddy, G.R.; Raju, B.D.P. NIR fluorescence spectroscopic investigations of Er³⁺-ions doped borate based tellurium calcium zinc niobium oxide glasses. *J. Lumin.* **2015**, *164*, 154–159. [[CrossRef](#)]
7. Gao, G.; Wei, J.; Shen, Y.; Peng, M.; Wondraczek, L. Heavily Eu₂O₃-doped yttria-aluminoborate glasses for red photoconversion with a high quantum yield: Luminescence quenching and statistics of cluster formation. *J. Mater. Chem. C* **2014**, *28*, 8678–8682. [[CrossRef](#)]
8. Bomfim, F.A.; Martinelli, J.R.; Kassab, L.R.P.; Wetter, N.U.; Neto, J.J. Effect of the ytterbium concentration on the upconversion luminescence of Yb³⁺/Er³⁺ co-doped PbO-GeO₂-Ga₂O₃ glasses. *Non-Cryst. Solids* **2008**, *354*, 4755–4759. [[CrossRef](#)]
9. Feng, L.; Wang, J.; Tang, Q.; Hu, H.; Liang, H.; Su, Q. Solids Optical properties of Er³⁺-singly doped and Er³⁺/Yb³⁺-codoped novel oxyfluoride glasses. *J. Non-Cryst.* **2006**, *352*, 2090–2095. [[CrossRef](#)]
10. Qi, C.; Hu, L.; Dai, S.; Jiang, Y.; Liu, Z. Spectra and lasing properties of Er³⁺, Yb³⁺:phosphate glasses. *Chin. Opt. Lett.* **2003**, *1*, 37–40.
11. Ji, Y.; Xiao, Y.; Huang, S.; Wang, W. Optical properties of Er³⁺ and Yb³⁺/Er³⁺-doped NaF-Na₂SO₄-Al(PO₃)₃ fluoro-sulfo-phosphate glasses. *Am. Ceram. Soc.* **2020**, *103*, 5664–5677. [[CrossRef](#)]
12. Pisarski, W.A.; Grobelny, Ł.; Pisarska, J.; Lisiecki, R.; Ryba-Romanowski, W. Spectroscopic properties of Yb³⁺ and Er³⁺ ions in heavy metal glasses. *J. Alloys Compd.* **2011**, *509*, 8088–8092. [[CrossRef](#)]
13. Shang, Z.; Ren, G.; Yang, Q.; Xu, C.; Liu, Y.; Zhang, Y.; Wu, Q. Spectroscopic properties of Er³⁺-doped and Er³⁺/Yb³⁺-codoped PbF₂-MO_x (M = Te, Ge, B) oxyfluoride glasses. *J. Alloys Compd.* **2008**, *460*, 539–543. [[CrossRef](#)]
14. Deopa, N.; Rao, A.S.; Gupta, M.; Prakash, G.V. Spectroscopic investigations of Nd³⁺ doped Lithium Lead Alumino Borate glasses for 1.06 μm laser applications. *Opt. Mater.* **2018**, *75*, 127–134. [[CrossRef](#)]
15. Hegde, V.; Wagh, A.; Hegde, H.; Vishwanath, C.S.D. Spectroscopic investigation on europium doped heavy metal borate glasses for red luminescent application. *Appl. Phys. A* **2017**, *12*, 1–13. [[CrossRef](#)]
16. Jadach, R.; Zmojda, J.; Kochanowicz, M.; Miluski, P.; Pisarska, J.; Pisarski, W.A.; Sołtys, M.; Lesniak, M.; Sitarz, M.; Dorosz, D. Investigation of the aluminum oxide content on structural and optical properties of germanium glasses doped with RE ions. *Spectrochim. Acta Part A Mol. Biomol. Spectrosc.* **2018**, *201*, 143–152. [[CrossRef](#)]
17. Dias, J.D.M.; Melo, G.H.A.; Lodi, T.A.; Carvalho, J.O.; Filho, P.F.F.; Barboza, M.J.; Steimacher, A.; Pedrochi, F. Thermal and structural properties of Nd₂O₃-doped calcium boroaluminate glasses. *J. Rare Earths* **2016**, *34*, 521–528. [[CrossRef](#)]
18. Rani, S.; Sanghi, S.; Ahlawat, N.; Agarwal, A. Influence of Bi₂O₃ on thermal, structural and dielectric properties of lithium zinc bismuth borate glasses. *J. Alloys Compd.* **2014**, *597*, 110–118. [[CrossRef](#)]
19. Doweidar, H.; Saddeek, Y.B. FTIR and ultrasonic investigations on modified bismuth borate glasses. *J. Non-Cryst. Solids* **2009**, *355*, 348–354. [[CrossRef](#)]

20. Pascuta, P.; Pop, L.; Rada, S.; Bosca, M.; Culea, E. The local structure of bismuth borate glasses doped with europium ions evidenced by FT-IR spectroscopy. *J. Mater. Sci. Mater. Electron.* **2008**, *19*, 424–428. [[CrossRef](#)]
21. Carnall, W.T.; Fields, P.R.; Rajnak, K. Electronic Energy Levels in the Trivalent Lanthanide Aquo Ions. I. Pr^{3+} , Nd^{3+} , Pm^{3+} , Sm^{3+} , Dy^{3+} , Ho^{3+} , Er^{3+} , and Tm^{3+} . *J. Chem. Phys.* **1968**, *49*, 4424–4442. [[CrossRef](#)]
22. Linganna, K.; Rathaiiah, M.; Vijaya, N.; Basavapoornima, C.; Jayasankar, C.K.; Ju, S.; Han, W.T.; Venkatramu, V. 1.53 μm luminescence properties of Er^{3+} -doped K–Sr–Al phosphate glasses. *Ceram. Int.* **2015**, *41*, 5765–5771. [[CrossRef](#)]
23. Burtan-Gwizdala, B.; Reben, M.; Cisowski, J.; Szpil, S.; Yousef, E.S.; Lisiecki, R.; Grelowska, I. Thermal and spectroscopic properties of Er^{3+} -doped fluorotellurite glasses modified with TiO_2 and BaO . *Opt. Mater.* **2020**, *107*, 109968. [[CrossRef](#)]
24. Swetha, B.N.; Devarajulu, G.; Keshavamurthy, K.; Jagannath, G.; Deepa, H.R. Enhanced 1.53 μm emission of Er^{3+} in nano-Ag embedded sodium-boro-lanthanate glasses. *J. Alloys Compd.* **2021**, *856*, 158212. [[CrossRef](#)]
25. Wu, L.; Zhou, Y.; Zhou, Z.; Cheng, P.; Huang, B.; Yang, F.; Li, J. Effect of silver nanoparticles on the 1.53 μm fluorescence in $\text{Er}^{3+}/\text{Yb}^{3+}$ codoped tellurite glasses. *J. Opt. Mater.* **2016**, *57*, 185–192. [[CrossRef](#)]
26. Judd, B.R. Optical absorption intensities of rare-earth ions. *Phys. Rev.* **1962**, *127*, 750–761. [[CrossRef](#)]
27. Ofelt, G.S. Intensities of crystal spectra of rare-earth ions. *J. Chem. Phys.* **1962**, *37*, 511–520. [[CrossRef](#)]
28. Li, Y.; Dou, B.; Xiao, Z.; Li, B.; Huang, F.; Li, Y.; Xu, S. Visible-infrared luminescence of Er^{3+} -doped fluorotellurite glasses. *Opt. Mater.* **2020**, *105*, 109900. [[CrossRef](#)]
29. Mariyappan, M.; Arunkumar, S.; Marimuthu, K. Judd-Ofelt analysis and NIR luminescence investigations on Er^{3+} ions doped $\text{B}_2\text{O}_3\text{--Bi}_2\text{O}_3\text{--Li}_2\text{O--K}_2\text{O}$ glasses for photonic applications. *Phys. B Condens. Matter.* **2019**, *572*, 27–35. [[CrossRef](#)]
30. Luewarasirikul, N.; Chanthima, N.; Tariwong, Y.; Kaewkhao, J. Erbium-doped calcium barium phosphate glasses for 1.54 μm broadband optical amplifier. *Mater. Today Proc.* **2018**, *5*, 14009–14016. [[CrossRef](#)]
31. Zhang, Y.; Xiao, Z.; Lei, H.; Zeng, L.; Tang, J. $\text{Er}^{3+}/\text{Yb}^{3+}$ co-doped tellurite glasses for optical fiber thermometry upon UV and NIR excitations. *J. Lumin.* **2019**, *212*, 61–68. [[CrossRef](#)]
32. Basavapoornima, C.; Linganna, K.; Kesavulu, C.R.; Ju, S.; Kim, B.H.; Han, W.T.; Jayasankar, C.K. Spectroscopic and pump power dependent upconversion studies of Er^{3+} -doped lead phosphate glasses for photonic applications. *J. Alloys Compd.* **2017**, *699*, 959–968. [[CrossRef](#)]
33. Zhao, Z.; Zhang, B.; Gong, Y.; Ren, Y.; Huo, M.; Wang, Y. Concentration effect of Yb^{3+} ions on the spectroscopic properties of high-concentration $\text{Er}^{3+}/\text{Yb}^{3+}$ co-doped phosphate glasses. *J. Mol. Struct.* **2020**, *1216*, 128322. [[CrossRef](#)]
34. Linganna, K.; Agawane, G.L.; In, J.H.; Park, J.; Choi, J.H. Spectroscopic properties of $\text{Er}^{3+}/\text{Yb}^{3+}$ co-doped fluorophosphate glasses for NIR luminescence and optical temperature sensor applications. *J. Ind. Eng. Chem.* **2018**, *67*, 236–243. [[CrossRef](#)]
35. Linganna, K.; Narro-García, R.; Manasa, P.; Desirena, H.; de la Rosa, E.; Jayasankar, C.K. Effect of BaF_2 addition on luminescence properties of $\text{Er}^{3+}/\text{Yb}^{3+}$ co-doped phosphate glasses. *J. Rare Earths* **2018**, *36*, 58–63. [[CrossRef](#)]
36. Langar, A.; Bouzidi, C.; Elhouichet, H.; Férid, M. Er–Yb codoped phosphate glasses with improved gain characteristics for an efficient 1.55 μm broadband optical amplifiers. *J. Lumin.* **2014**, *148*, 249–255. [[CrossRef](#)]
37. Basavapoornima, C.; Maheswari, T.; Depuru, S.R.; Jayasankar, C.K. Sensitizing effect of Yb^{3+} ions on photoluminescence properties of Er^{3+} ions in lead phosphate glasses: Optical fiber amplifiers. *Opt. Mater.* **2018**, *86*, 256–269. [[CrossRef](#)]